Published in final edited form as:
Biochemistry. 2011 May 24; 50(20): 4371–4381. doi:10.1021/bi200031m.

A cleavage enzyme - cytometric bead array provides biochemical profiling of resistance mutations in HIV-1 Gag and protease†

Sebastian Breuer[‡], **Homero Sepulveda**[§], **Yu Chen**[§], **Joseph Trotter**[§], and **Bruce E. Torbett**[‡,*]

[‡] Department of Molecular and Experimental Medicine, The Scripps Research Institute, CA, 92037, USA

[§] BD Biosciences, 10975 Torreyana Road, San Diego, CA 92121-1106, USA

Abstract

The majority of protease – substrate assays rely on short, synthetic peptide substrates consisting of native or modified cleavage sequences. These assays are inadequate for interrogating the contribution of native substrate structure distal to a cleavage site that influences enzymatic cleavage or for inhibitor screening of native substrates. Recent evidence from HIV-1 isolates obtained from individuals resistant to protease inhibitors has demonstrated that mutations distal to or surrounding the protease cleavage sites in the Gag substrate contribute to inhibitor resistance. We have developed a protease – substrate cleavage assay, termed the Cleavage Enzyme – Cytometric Bead Array (CE-CBA), which relies on native domains of the Gag substrate containing embedded cleavage sites. The Gag substrate is expressed as a fluorescent reporter fusion protein and substrate cleavage can be followed through the loss of fluorescence utilizing cytometry. The CE-CBA allows precise determination of alterations in protease catalytic efficiency (k_{cat}/K_M) imparted by protease inhibitor resistance mutations in protease and/or *gag* in cleavage or non-cleavage site locations in the Gag substrate. We show that the CE-CBA platform can identify HIV-1 protease present in cellular extractions and facilitates the identification of small molecule inhibitors of protease or its substrate Gag. Moreover, the CE-CBA can be readily adapted to any enzyme – substrate pair and can be utilized to rapidly provide assessment of catalytic efficiency as well as systematically screen for inhibitors of enzymatic processing of substrate.

Proteases are enzymes that catalyze the hydrolysis of peptide bonds in many key physiological processes in most organisms and pathogens. Approximately 2 % of the human and mouse genomes are predicted to encode proteases (1, 2). Inappropriate proteolysis is involved in inflammation, neurodegenerative diseases, cancer, and parasite pathogenesis (3). Furthermore, bacteria and viruses have unique proteolytic pathways necessary for their lifecycles and in human pathogens these pathways are amenable to small molecule targeting

†The studies were supported by funds from NIH, GM083658, GM48870, and AI4081585, to B.E.T.. S.B. was supported by CHRP-F09-SRI-205. CFAR support, 3 P30 AI036214-13S1, is gratefully acknowledged.

*Address correspondence to B.E.T. Phone: +1 858.784.9123; Fax: +1 858.784.7714; betorbet@scripps.edu.

SUPPORTING INFORMATION AVAILABLE

The validation of recombinant GST fusion proteins and the anti-GST antibody by SDS PAGE, western blot and MALDI MS; the characterization of binding between GST-X-mV and anti-GST antibody labeled beads and establishment of a strepavidin-based bead and fusion protein platform; the time course of protease-mediated cleavage of GST-X-mV containing either a HIV- 1 PR or a thrombin cleavage site; the IC_{50} determinations of amprenavir and pepstatin A; and the analysis of the robustness of a multiplexed HTS CE-CBA. This material is available free of charge via the Internet at http://pubs.acs.org

(2-4). Inhibitors to HIV-1 protease (PIs) are a component of Highly Active Anti-Retroviral Therapy (HAART), the standard treatment for HIV-1-infected individuals (3-5).

PIs are effective in reducing viral burden, thereby slowing or halting the progression to Acquired Immune Deficiency Syndrome (AIDS) (5). PIs target the 99 amino acid aspartyl protease homodimer, disrupting the multi-step, enzymatic processing of the Gag-Pol polyprotein substrate, which is required for HIV maturation (6). However, over time, PI (drug) resistant viruses can emerge during HAART (7, 8). PI resistance is the result of initial PR active site mutations, which decreases the inhibitor affinity. These primary mutations are followed by compensatory mutations distal to the active site, which improves protease catalytic efficiency, k_{cat}/K_M (9, 10). In addition to PR mutations enhancing drug resistance, viruses obtained from HAART experienced individuals have mutations in *gag* at protease cleavage sites (CS) as well as in *gag* non-cleavage site (NCS) locations (11-13). Some of the *gag* cleavage site mutations improve the catalytic efficiency of both wild type protease and drug-resistant proteases (10, 14, 15). In contrast to the mutations in cleavage sites, the resistances mechanisms resulting from non-cleavage site mutations are less well understood.

Currently, the method of choice for estimating k_{cat}/K_M values for protease processing relies on the use of short, usually 8-12 amino acids in length, synthetic peptides corresponding to cleavage sites, or their derivatives altered in chemical structure, as substrates (9, 16). The HIV-1 PR hydrophobic cavity can hold up to 8 amino acids of substrate bound in an extended β-sheet conformation through extensive hydrogen bond and van der Waal interactions (17). PR cleavage activity is monitored using fluorogenic substrates or high-pressure liquid chromatography (HPLC) (18, 19). Fluorogenic substrate assays (FSA) have been extremely useful for assessing the biochemical role of both PI-mediated mutations in PR and *gag* cleavage sites (20). However, the precise, role of distal (11, 15, 21) and non-cleavage site (12) *gag* mutations in regards to protease function and PI resistance have proven more problematic, since these mutations are not present in and lie distal to the 8-10 amino acid sequences used for peptide substrates. Moreover, techniques like SDS PAGE when used in conjunction with Western Blot are suitable for the analysis of large protease substrates, but are low throughput and considered limited in quantitative precision.

Herein we report on our development of a HIV-1 protease – substrate cleavage assay, termed cleavage enzyme – cytometric bead array (CE-CBA), that overcomes some of the limitations of established technologies which utilize short, protease substrates or PAGE-based methods for cleavage quantification. The CE-CBA provides a cleavage enzyme – native substrate assay platform adaptable to any enzyme - substrate combination. The HIV-1 protease substrates developed for use are native Gag domains containing embedded cleavage sites and are expressed as fluorescent fusion proteins. A limitation of past bead-based approaches for biochemical analyses of protease - substrate cleavage was the compression of dynamic range for quantifying substrate cleavage and assay sensitivity to substrate concentrations (22). We have fully optimized signal to noise assessment of substrates for high fidelity and throughput, which allows rapid and precise analysis of enzyme kinetics.

Materials and Methods

Plasmid Construction and Subcloning

The vector pGex4G-mVenus was derived from the pGex4T2 vector (GE Healthcare, Piscataway, NJ) and generated by an exchange of the thrombin site to a 4 amino acid glycine linker by site directed mutagenesis. The mVenus gene was inserted using the *EcoRI* and *XhoI* restriction sites. In order to extend the upstream multiple cloning site (MCS) of pGex4G-mVenus, we extended the MCS through the addition of an *NdeI* site. Next, the mVenus sequence was mutated at A206K to disrupt potential dimerization. For inclusion of

gag and fragments of *gag*, the *NdeI* and *EcoRI restriction sites* were used for cloning. All substitutions were generated using the QuickChange site directed mutagenesis kit (Stratagene, Santa Clara, CA). All 8 amino acid cleavage sites were generated by overlap extension PCR. All generated plasmids were confirmed by sequencing.

Protein Expression and Purification

Proteins were synthesized using a bacterial expression system and standard affinity chromatography purification methods. Briefly, BL21DE3(pLysS) bacteria (Invitrogen, Carlsbad, CA) were transformed with the expression plasmid of interest according to manufacturer's protocol. Bacteria were grown to a density of OD_{600nm}= 0.8 in LB + 100 μg/ml ampicillin at 28 °C and then induced by adding 0.5 mM Isopropyl-beta-D-thiogalactospyranoside (IPTG). After 8 hrs the cells were harvested by centrifugation (6,000 g, 15 min), washed with buffer A (20 mM Tris-Hcl pH 8.0, 500 mM NaCl, 0.5 mM DTT and 0.5 % Tween-20), then lysed by lysozyme lysis combined with a French press. To avoid bacterial protease activity a protease inhibitor mix (Complete, Mini Protease inhibitor Tablets, Roche, Nutley, N.J.) plus pepstatin A (Sigma-Aldrich, St. Louis, MO) was added to the lysis buffer. After separation by centrifugation (30,000 g, 45 min) the supernatant was loaded onto a GSH column (GE Healthcare) and washed with buffer A with 20 column volumes. The protein was eluted by addition of 20 mM GSH in buffer A and the purity verified by SDS PAGE. The protein was concentrated using Amicon Ultra-15 filter devices (Millipore, Billerica, MA) with the appropriate cutoff. All proteins were confirmed by MALDI MS and fluorescence spectroscopy. The buffer of the proteins was exchanged via dialysis to the appropriate enzyme assay buffer. All purification steps were conducted at 4 °C.

Native PAGE and Fluorescence Quantification

For the native PAGE the NativePAGE Novex Bis-Tris gel system was used (Invitrogen). 5 μg of each protein sample were separated by PAGE and the fluorescence in the gel was detected by quantitative imaging using a Typhoon Trio gel scanner (GE Healthcare).

MALDI Mass Spectrometry

For the MALDI MS analysis 8 μM GST-MA-CA was incubated with 25 nM protease in 20 mM MES pH 6.0, 200 mM NaCl, 5 % glycerol at 37 °C. A MALDI TOF Voyager STR (Applied Biosystems, Carlsbad, California) and matrix (50 mg/ml sinapinic acid, 0.1 % TFA, 50 % acetonitrile) was used for the analysis.

Immobilization of Protein on Beads

The anti-GST antibody coated beads (BD Bioscience) were incubated with GST fusion protein for 1 hr at RT with mixing and the mixture was protected from light. The ratio of protein / beads was 1 - 100 pmol / 10,000 with the protein concentration at 0.01 μM during bead to protein coupling. To remove unbound protein from the bead-protein mixture, beads were washed 3 times by adding 500 μl PBS, 500 mM NaCl, 0.005 % DDM, with centrifugation (5,000 g, 5-10 min) to pellet beads. After the final centrifugation the beads were re-suspended in the appropriate buffer at a concentration of 200 beads/μl.

Determination of the enzyme kinetics by CE-CBA

Enzyme kinetic data were generated by monitoring the cleavage reaction as a function of enzyme concentration and the exponential equation $S_{(t)}/S_{(0)} = e^{-kobs*t}$ where $S_{(t)}$ is the concentration of the substrate remaining at the time t, $S_{(0)}$ is the initial substrate concentration and $k_{obs} = k_{cat}$*[enzyme] / K_M. The remaining fluorescence on the bead after protease treatment corresponds to the remaining substrate. The data were fitted with $F_{(t)}/F_{(0)}$

$= e^{-kobs*t} + F_{off}$ where $F_{(t)} = S_{(t)}$ and $F_{(0)} = S_{(0)}$ and F_{off} is the fluorescence offset utilizing Prism v5.0c (GraphPad Software, San Diego, CA) software. For the protease-mediated cleavage reaction the fusion protein was incubated with HIV-1 PR in 25 mM MES pH 5.5, 200 mM NaCl, 2.5 % glycerol, 0.005 % n-dodecyl beta-D-maltoside (DDM) at 25 °C or 37 °C. The cleavage reaction was stopped by adding 5 μM PI Darunavir (NIH AIDS Reagents Program) in 20 mM Tris-Hcl pH 8.0, 400 mM NaCl, 0.005 % (DDM).

The cleaved and uncleaved substrate were immobilized on beads, proteins bound through non-specific interaction were removed by a wash step using a Manifold vacuum device (Bio-Rad Laboratories, Hercules, CA) fitted with multiscreen-BV filter plates (Millipore). Bead fluorescence was determined by flow cytometry utilizing a FACSCanto II instrument outfitted with a HTS unit (BD Bioscience, San Jose, CA).

Experiments that required an exact substrate concentration were undertaken as described above, but without an immobilization step. Briefly, protease and substrate were mixed for the desired time period, beads with coupled antibody were added, cleaved and uncleaved substrate were captured, and then bead fluorescence was then determined by flow cytometry.

The enzyme concentrations were confirmed using active site titration. All reactions were carried out using concentrations of substrate well below K_M, where the appearance of the product is a pseudo-first order process. The k_{cat}/K_M values were calculated as described previously. All experiments were carried out according to the condition $[S] \ll K_M$.

Determination of the enzyme kinetics by Native PAGE-based PR – Gag cleavage assay

10 nM of the fusion protein was incubated with a dilution series of protease at 37 °C. After 30 min the reaction was stopped and the samples separated by Native PAGE and the fluorescence quantified by a Typhoon laser gel scanner. The condition $[S] \ll K_M$ was chosen as described previously.

Determination of the IC_{50} values - *CE-CBA*

All experiments involving protease inhibitors were performed using a buffer with additional 5 % DMSO. DMSO did not affect the integrity of the protein on the beads and did not interfere with the fluorescence signal in the flow cytometer. HIV-1 PR was adjusted to 1-25 nM and mixed with a dilution concentration series of protease inhibitor. Beads with a MA/CA cleavage site were added and incubated at 37 °C and stopped at a time point within the initial velocity phase of the enzymatic reaction. The reaction was terminated as previously described and beads were washed and analyzed by flow cytometry. The IC_{50} value was calculated by nonlinear regression of change in fluorescence as a function of PI concentration using either a 4 parameter logistic model or the quadratic equation (Morrison equation) by Origin 7.0 (23). All measurements were performed in duplicates and repeated in independent experiments. FSA: This assay was performed as previously reported (24). As a variation we used 25 mM MES pH 6.0, 200 mM NaCl, 2.5 % glycerol, 0.005 % DDM as the reaction buffer.

High-throughput screening and hit validation

Cytometric beads were labeled with GST-X-mV proteins containing Gag substrates, thrombin cleavage site or a control without a cleavage site, as described previously. The cleavage reaction was carried out in 100 μl volume containing 50 μM compound, 50 nM HIV-1 PR or 0.01 U/μl thrombin, 5 % DMSO at 37 °C for 1 hr in 96-well plates. The reaction with HIV-1 PR was performed in 25 mM MES pH 6.0, 200 mM NaCl, 2.5 % glycerol, 0.005 % DDM separately from thrombin in 50 mM Tris-HCL pH 8.4, 200 mM

NaCl, 2.5 mM CaCl2. After 1 hr the reaction was stopped by removing the beads from HIV-1 PR or thrombin through the use of filter plates, as described above, or by adding PI, then beads were pooled and analyzed by flow cytometry. For the validation of positive hits from the screen 50 μM of the compounds were used and compared to 50 μM amprenavir and miconazole in a multiplexed CE-CBA.

In vivo cleavage reaction of HIV-1 tissue culture supernatant derived proteases

HIV-1 infected SUP-T1 cells were infected and cultured as previously described (24). After 3 days the culture supernatant was removed and the cells were lysed with a lysis buffer (Promega). After clearing the lysate by centrifugation, the supernatant was tested for PR activity in a monoplex CE-CBA.

Confocal imaging of beads

Beads were derived as described previously and analyzed using a BD Pathway 435 Bioimaging System (BD Biosciences).

Results

Design of a robust fusion protein scaffold for expressing substrates

Advancements in cytometric bead chemistry allow fluorescently-labeled proteins to be coupled to polystyrene cytometric beads for assessment of protein-protein interactions or enzyme function utilizing flow cytometry (22, 25, 26). The CE-CBA utilizes a fusion protein scaffold composed of an N-terminal anchor, which can be coupled to cytometric beads, followed by the insertion site, X, suitable for expression of protease substrates and a C-terminal fluorescent reporter (Figure 1a). Anchor and fluorescence domains were produced from sequentially encoded gene sequences, which allow the synthesis of various protease substrates, thereby reducing reagent costs and preparation time. The tandem anchor – substrate fluorescent reporter protein synthesis provides for consistent protein labeling and increases quality control in comparison to substrate assays where reporters are chemically coupled to substrate. The arrangement of an encoded protease substrate between the anchor and fluorescent reporter was designed so as to expand the utility of the CE-CBA for screening for novel protease activity since any sequence can be encoded at X. The glutathione S-transferase (GST) anchor protein was selected for use given its demonstrated properties of promoting folding and the stabilization of fusion proteins (27). mVenus, a derivate of the green fluorescence protein, was chosen as the reporter given its accepted use in many biological systems (28-30). Additionally, the spectral features of mVenus, such as enhanced brightness, broad excitation spectrum, as well as the low dimerization tendency, were necessary to develop the CE-CBA (28-30). As shown in Figure 1a, HIV-1 proteins can be expressed within the GST-X-mVenus (GST-X-mV) reporter fusion protein, where X represents either Gag domains that contain one endogenous cleavage site or an 8 amino acid peptide cleavage site. Herein, we refer to Gag substrates as a GST-X-mV fusion protein containing two full-length Gag domains (e.g. MA and CA) with one endogenous, embedded cleavage site. All linker regions of the GST-X-mV protein scaffold were engineered to be resistant to protease activity. Mass spectrometry confirmed that HIV PR cleaved full-length Gag domains correctly with protease processing restricted to Gag cleavage sites (Supplementary Figure 1a,b and c), with Gag cleavage patterns similar to that reported from viral extracts (31).

To attach the GST-X-mV fusion protein to the cytometric beads, monoclonal anti-GST antibodies are first chemically coupled to the beads, followed by anti-GST antibody binding of GST-X-mV. The anti-GST antibody was resistant to protease cleavage (Supplementary Figure 1d). The use of high-affinity, anti-GST antibody to immobilize GST-X-mV to beads

is rapid, promotes directionality, and does not require the additional step of biotinylation of the purified protein or GSH separation for rebinding to GSH-labeled beads. Optimization of chemical coupling of anti-GST antibodies to beads and GST-X-mV capture by bead-bound antibodies is fully discussed in Supplementary Figure 2a,b. When GST-p2/NC_{CS}-mV was attached to beads, then viewed by confocal laser scanning microscopy, a uniform distribution of fluorescence on the bead surface without overt protein aggregation was evident (Figure 1b). To extend the CE-CBA platform technology to conditions where antibody use is limiting, such as under reducing conditions, we have established a different affinity matrix, strepavidin tag II-X-mV to strepavidin on beads, as discussed in Supplementary Figure 2c,d.

To monitor changes in the fluorescence on the bead surface by flow cytometry a FACSCanto II was utilized in combination with an orthogonal plate reader for precise, high-throughput analysis. To determine relative changes in bead fluorescence for enzyme kinetic evaluation we defined baseline fluorescence (0 %) using the intrinsic bead fluorescence as shown in Figure 1c,d. In order to obtain the relative fluorescence intensity values for GST-X-mV attached to beads the median and percentage of robust coefficient of variation was determined.

Two different strategies for CE-CBA assessment of Gag substrate processing by protease were developed and evaluated (Figure 1c,d). The on bead assay requires that the GST-X-mV fusion protein first be attached to the beads before protease processing. When protease is added the GST-X-mV fusion protein is processed at the correct cleavage site liberating mVenus (Figure 1c). A related methodology based on direct coupling to beads, but not based on coupling of high affinity capture antibodies to beads, has been utilized to evaluate enzymatic cleavage of the anthrax lethal factor, Factor Xa, and botulinum neurotoxin Type A (22). Our in solution assay relies on the protease first processing the GST-X-mV fusion protein in solution. After a defined period of processing time, beads coupled with anti-GST antibody are then added and the mixture containing uncleaved GST-X-mV and cleaved GST-X are captured (Figure 1d). In both methodologies the loss mVenus fluorescence is correlated with protease-mediated processing of Gag substrates and can be quantified by flow cytometry. We first evaluated on bead protease cleavage of bead bound GST-p2-NC-mV (Figure 1c). However, we found that cleavage of the bead-bound Gag substrates, such as GST-p2-NC-mV, when incubated with saturating amounts of protease was not complete (Figure 1c). This finding has been reported previously for methodologies where the substrate is first coupled to beads before enzyme addition (22). In contrast to the findings for on bead processing analysis, Figure 1c, the in solution processing analysis increases the dynamic range of cleaved product readout by approximately a log, as seen in Figure 1d. The in solution CE-CBA methodology can be used for any protease - GST-X-mV pair (Figure 1a) and was the method of choice for further evaluation of enzyme kinetics.

To confirm the specificity of the in solution CE-CBA to analyze protease processing of Gag domains, wild type matrix-capsid GST-MA-CA-mV, and the Y132I cleavage site matrix-capsid mutant GST-MA-CA(Y132I)-mV, were compared (Figure 1a). A recent report demonstrated that the Y132I mutation in the matrix-capsid cleavage site disrupts PR processing, resulting in loss of HIV-1 maturation and viral infectivity (32). Similarly, utilizing the in solution CE-CBA to analyze PR processing of wild type GST-MA-CA-mV, and the cleavage site mutant GST-MA-CA(Y132I)-mV, the single amino acid change from Y (⇒) I disrupted GST-MA-CA-mV processing by PR (Figure 2b,c). Thus, a single cleavage site mutation known to disrupt viral processing specifically disrupts GST-MA-CA-mV processing. In addition, incubation of the GST-MA/CA_{cs}-mV fusion protein with the proteolytic enzyme thrombin, a necessary protease in human blood coagulation, showed no

cleavage acitivity, indicating enzyme -cleavage site fidelity of the tested Gag substrates (Supplementary Figure 3a,b).

We next evaluated whether HIV-1 protease activity could be detected from whole cellular extracts from HEK 293T cells transiently expressing Gag-Pol. As seen in Figure 2d cellular extracts resulted in comparable GST-MA/CA_{cs}-mV cleavage to that resulting from recombinant PR (Figure 2d). Cellular extract from cells not transiently expressing Gag-Pol demonstrated no GST-MA/CA_{cs}-mV cleavage activity (Figure 2d). These results demonstrate that the CE-CBA has the capacity to detect HIV-1 protease activity from cellular isolates.

Characterization of Gag substrate cleavage sites

To validate in solution CE-CBA-based analyses of PR processing of Gag substrates, a variety of Gag proteins and cleavage sites were evaluated and kinetic values determined. A representative experiment determining catalytic efficiency, k_{cat}/K_M, of GST-MA/CA_{cs}-mV and GST-MA-CA-mV cleavage by protease is displayed in Figure 3. k_{cat}/K_M was calculated by fitting the consumption of substrate as a function of enzyme concentration and time. Catalytic efficiency for GST-MA/CA_{cs}-mV was 40.5 ± 1.4 $mM^{-1}s^{-1}$, whereas for GST-MA-CA-mV it was 12.4 ± 1.1 $mM^{-1}s^{-1}$. PAGE-based cleavage efficiency quantification of GST-MA/CA_{cs}-mV cleavage by protease (Figure 3b,d) showed a similar catalytic efficiency value, 46.6 ± 0.5 $mM^{-1}s^{-1}$, as that obtained from in solution CE-CBA analysis, 40.5 ± 1.4 $mM^{-1}s^{-1}$, which is similar to reported values (9). These findings confirm that k_{cat}/K_M determination was dependent on the GST-MA/CA_{cs}-mV fusion protein and independent of the method of quantification.

PR inhibitor resistance mutations can impart dramatic effects on enzymatic processing and alterations in catalytic efficiency (16, 33, 34). The I84V PR mutation is found in HIV-1 obtained from individuals after treatment with PIs and arises in virus after PI selection in tissue culture (16, 35). The I84V PR mutation provides PI resistance and results in decreased enzymatic activity (16). To determine whether in solution CE-CBA can quantify alterations in enzymatic activity, k_{cat}/K_M was determinedfor both wild type and mutant I84V PR with GST-MA/CA_{cs}-mV as substrate. Wild type PR was found to be 1.9-fold more enzymatically active than the I84V PR (Figure 3c,d), thus confirming that the I (⇒) V mutation affects k_{cat}/K_M, in a range similar, 2.2 fold, to that reported by Muzammil et. al. (36).

Assessment of protease inhibitor potency, protease inhibitor resistance, and screening for new inhibitors has been aided through the use of FSA (24). Since FSA is the standard methodology for obtaining IC_{50} values for protease inhibitors, we evaluated and found that CE-CBA produced similar IC_{50} values as FSA for amprenavir, a clinical HIV-1 protease inhibitor, and pepstatin A, an aspartyl peptidase inhibitor (Supplementary Figure 4).

Enzymatic analysis of protease inhibitor resistant gag mutations

The known PI resistance *gag* cleavage site mutations, NC-p1(A431V) and p1-p6(L449F), have been implicated in enhancing PR processing through alterations of k_{cat}/K_M (9, 19). Generally, *gag* cleavage site mutations are amenable to kinetic analyses utilizing small synthetic peptide substrate assays. In contrast, biochemical assessment of the distal cleavage site NC-p1(K436E,I437V) mutation and non-cleavage site mutations like p1-p6(T456S) have mostly relied on gel electrophoresis based quantification of Gag isolated from virally infected cells (11, 37). Although gel electrophoresis can provide information as to whether the mutations increase cellular Gag abundance over time, such as reported for the NC-p1(K436E,I437V) mutations, the methodology does not easily lend itself to determination of k_{cat}/K_M (11).

We first evaluated whether the in solution CE-CBA could quantify alterations in k_{cat}/K_M when the wild type PR or the enzymatically less active I84V mutant PR and the wild type Gag domain or Gag domain containing the cleavage site mutations NC-p1(A431V) and p1-p6(L449F) were analyzed. The presence of either *gag* cleavage site mutation increased the k_{cat}/K_M of wild type PR, 2.2-fold, NC-p1(A431V), or 4.4-fold, p1-p6(L449F) (Figure 4a,b and Supplementary Table 1), and increased the relative rate of Gag cleavage (Supplementary Table 1), as compared to the wild type Gag. When wild type NC-p1 or p1-p6 Gag domains and I84V PR were analyzed, cleavage efficiency was found to be 70 % less, NC-p1, and 80% less, p1-p6, as compared to wild type PR with the same Gag domains (Figure 4a,b and Supplementary Table 1). In contrast, when the mutant Gags and the I84V PR were analyzed, we found that the NC-p1(A431V) mutation restored catalytic efficiency to 80 % of that of wild type PR, whereas p1-p6(L449F) restored catalytic efficiency to 100 % of that of wild type PR (Supplementary Table 1).

We next assessed the role of *gag* distal cleavage site NC-p1(K436E,I437V) mutation and the non-cleavage site mutation p1-p6(T456S), as compared to wild type *gag*, in altering k_{cat}/K_M values. As can be seen in Figure 4c, and summarized in Supplementary Tables 1, the presence of the mutations enhanced the catalytic efficiency approximately 3.2-fold and increased the relative cleavage rate, 5.7-fold, over wild type Gag (Supplementary Table 2). Moreover, the non-cleavage site mutation p1-p6(T456S) altered the catalytic efficiency 2-fold (Figure 4d and Supplementary Table 1). These findings confirmed that the non-cleavage site mutation T456S, provided enhancement of catalytic efficiency and emphasized the importance of distal site mutations in resistance (37).

Lastly, we evaluated whether the NC-p1 or p1-p6 *gag* mutant series would confer increases in amprenavir IC_{50}s, as compared to wild type Gag substrate domains, thereby accounting for the reported PI resistance (9, 19). The amprenavir IC_{50} values revealed by CE-CBA showed similar IC_{50}s for the wild type NC-p1 and p1-p6 mutants, indicating that that cleavage site and distal cleavage site mutations in *gag* did not confer PI resistance, per se (Figure 4 and Supplementary Table 3) (11). Therefore, as has been suggested in the literature and confirmed by our results, the PI resistance provided by the NC-p1 or p1-p6 *gag* mutant series relies on alterations in protease catalytic efficiency, rather than alterations in PI affinity (9, 11).

The potential of parallel monitoring and high-throughput screening utilizing CE-CBA

Parallelization and miniaturization in an orthogonal readout format are essential steps in high-throughput screening (HTS) (38). The usage of 96-well or 384-well plates with the capacity of CE-CBA for multiplexing and high-throughput assessment provides an ideal format for screening for small molecules that inhibit Gag cleavage (Figure 5). To this end, we tested the capacity of CE-CBA to multiplex in a pilot experiment with 4 bead positions bar-coded by the intrinsic red-fluorophore bead fluorescence. The two upper positions in the bivariant plot in Figure 5a represent beads coupled with the Gag substrates GST-MA-CA-mV or GST-CA-p2-mV. The two lower bead populations are irrelevant proteins for monitoring off-target activity during the screening for small molecules that disrupt Gag substrate cleavage. In this example, the beads present in the third position were coupled with GST-Thr_{CS}-mV, containing the thrombin cleavage site, which serves as a control for non-specific HIV-1 PR cleavage. As a control for non-specific cleavage or compound activity, a closely related cleavage site of the enzyme being evaluated may be more appropriate, i.e., for HIV-1 PR, human aspartyl protease BACE-1 or Renin and their substrates could be utilized (4). The bivariant dot blot indicates a decreased fluorescence (shift to the left) on beads, indicating cleavage of each distinct substrate. The two controls were not affected by HIV-1 PR, thus indicating PR specificity. Moreover, each Gag substrate serves as a control for the other in regards to the specificity of the inhibitor. That is, the cleavage - substrate

inhibition pattern allows the determination of the action of each inhibitor. For example, a general inhibitor of protease function would reduce cleavage of both Gag substrates, where as a specific Gag substrate inhibitor would disrupt the cleavage of only substrate. Inhibitors with a promiscuous activity will disrupt all cleavage reactions (Figure 5c). As can be seen in Supplementary Figure 5, CE-CBA is adaptable to a miniaturized, 20 μl sample volume format, and displayed screening robustness as shown by the statistical Z′-factor of 0.837 ± 0.003 (mean ± s.e.m.) (39). We screened a combinatorial library of ~ 340 small compounds using a multiplexed CE-CBA with two Gag substrates and one control protein without a HIV-1 protease cleavage site. The screen identified one compound with specific protease inhibitor activity (Figure 5 b,c). The PI amprenavir and the antifungal agent miconazole, a promiscuous inhibitor, exemplified the two profiles of a specific (amprenavir) and an unspecific (miconazole) inhibitor. Thus, the multiplexed CE-CBA increases the information content obtained per well, providing fast profiling of small molecule specificity and potency.

Discussion

A bead-based cytometric technique has been developed for fast and precise profiling of enzymatic activity of wild type and drug-resistant proteases and their substrates. The use of cleavage sites embedded in native domains allows the Gag structure outside of the minimal cleavage site to regulate cleavage activity. Moreover, due to the configuration of the GST-Gag-mVenus platform, the cleavage readout is robust, with good signal-to-noise fluorescence, which allows the CE-CBA to be utilized for interrogation of drug resistance mutations present in Gag and high-throughput inhibitor screening. The assay is based on a 96-well or 384-well plate platform, easily configurable to high-throughput screening, and is suitable for multiplexing applications. The CE-CBA advances current bead-based methodologies (22).

The ability to evaluate enzymatic processing of cleavage sites embedded within the Gag domain, or any enzyme – full- or partial-length substrate pair for that matter, allows the protein structure surrounding the cleavage site to dictate cleavage conformation and to be assessed in the CE-CBA. This aspect of the CE-CBA cannot be accomplished in commonly employed methodologies where minimal cleavage site substrates are utilized (40). As shown, we have demonstrated the use of CE-CBA to evaluate non-cleavage site and distal cleavage site mutations in Gag and confirmed their contribution to HIV-1 clinical drug resistance.

Proteases have become an important area of investigation in academic and pharmaceutical research given protease's relevance in viral or bacterial infections, cancer, neurodegenerative diseases and many other pathophysiological processes in humans (3). Here, the use of CE-CBA and substrates containing embedded cleavage sites allows investigation of the protein structure surrounding the cleavage site for mechanistic evaluation and small molecule screening (3). Given the ease of substrate production, CE-CBA can be a useful and efficient platform to screen a vast number of unknown protease cleavage sites in combinatorial fashion. Furthermore, based on our cellular studies utilizing ectopically expressed protease, the CE-CBA can be readily adaptable to assess proteases directly from cells.

Multiplexing and HTS are a common trend for drug discovery efforts. Emergence of promiscuous inhibitors as well as compound related artifacts constitute a major challenge in drug discovery (38, 41). The CE-CBA provides the flexibility for small molecule probing of complex substrate combinations in a high-throughput fashion. Moreover, we show that CE-CBA multiplexing provides a potential methodology for identifying small molecule inhibitors of substrate cleavage, while reducing false positives. The CE-CBA will be useful

for identification of inhibitors that bind to and disrupt Gag processing, a direction we are currently undertaking.

In summary, our studies demonstrate the applicability of the CE-CBA technology for evaluating changes in catalytic efficiency of HIV-1 protease and/or Gag resulting from drug resistance mutations. The methodology will be useful for high-throughput screening of small molecules that disrupt HIV-1 protease cleavage of Gag. Moreover, given the flexibility of the CE-CBA it should be readily adaptable for interrogation of any enzyme – substrate combination.

Supplementary Material

Refer to Web version on PubMed Central for supplementary material.

Acknowledgments

We are grateful to Drs. Ying C. Lin, John Elder, Max Chang, and Michael Giffin for providing HIV-1 protease and for helpful discussions and Daniel Kuhna for providing valuable technical expertise during the cloning and purification of Gag fusion proteins, Jeanne Elia for help with confocal imaging. We thank Drs. Diether Recktenwald, M.G. Finn, Karin Staflin and Maureen Goodenow for critical reading of the manuscript. This is publication MEM #20781 from The Scripps Research Institute.

References

1. Rawlings ND, Tolle DP, Barrett AJ. MEROPS: the peptidase database. Nucleic Acids Res. 2004; 32:D160–164. [PubMed: 14681384]
2. Puente XS, Sanchez LM, Overall CM, Lopez-Otin C. Human and mouse proteases: a comparative genomic approach. Nat Rev Genet. 2003; 4:544–558. [PubMed: 12838346]
3. Turk B. Targeting proteases: successes, failures and future prospects. Nat Rev Drug Discov. 2006; 5:785–799. [PubMed: 16955069]
4. Abbenante G, Fairlie DP. Protease inhibitors in the clinic. Med Chem. 2005; 1:71–104. [PubMed: 16789888]
5. Flexner C. HIV drug development: the next 25 years. Nat Rev Drug Discov. 2007; 6:959–966. [PubMed: 17932493]
6. Colonno R, Rose R, McLaren C, Thiry A, Parkin N, Friborg J. Identification of I50L as the signature atazanavir (ATV)-resistance mutation in treatment-naive HIV-1-infected patients receiving ATV-containing regimens. J Infect Dis. 2004; 189:1802–1810. [PubMed: 15122516]
7. Zennou V, Mammano F, Paulous S, Mathez D, Clavel F. Loss of viral fitness associated with multiple Gag and Gag-Pol processing defects in human immunodeficiency virus type 1 variants selected for resistance to protease inhibitors in vivo. J Virol. 1998; 72:3300–3306. [PubMed: 9525657]
8. Condra JH, Schleif WA, Blahy OM, Gabryelski LJ, Graham DJ, Quintero JC, Rhodes A, Robbins HL, Roth E, Shivaprakash M, et al. In vivo emergence of HIV-1 variants resistant to multiple protease inhibitors. Nature. 1995; 374:569–571. [PubMed: 7700387]
9. Feher A, Weber IT, Bagossi P, Boross P, Mahalingam B, Louis JM, Copeland TD, Torshin IY, Harrison RW, Tozser J. Effect of sequence polymorphism and drug resistance on two HIV-1 Gag processing sites. Eur J Biochem. 2002; 269:4114–4120. [PubMed: 12180988]
10. Nijhuis M, Schuurman R, de Jong D, Erickson J, Gustchina E, Albert J, Schipper P, Gulnik S, Boucher CA. Increased fitness of drug resistant HIV-1 protease as a result of acquisition of compensatory mutations during suboptimal therapy. AIDS. 1999; 13:2349–2359. [PubMed: 10597776]
11. Nijhuis M, van Maarseveen NM, Lastere S, Schipper P, Coakley E, Glass B, Rovenska M, de Jong D, Chappey C, Goedegebuure IW, Heilek-Snyder G, Dulude D, Cammack N, Brakier-Gingras L, Konvalinka J, Parkin N, Krausslich HG, Brun-Vezinet F, Boucher CA. A novel substrate-based

HIV-1 protease inhibitor drug resistance mechanism. PLoS Med. 2007; 4:e36. [PubMed: 17227139]

12. Ho SK, Coman RM, Bunger JC, Rose SL, O'Brien P, Munoz I, Dunn BM, Sleasman JW, Goodenow MM. Drug-associated changes in amino acid residues in Gag p2, p7(NC), and p6(Gag)/p6(Pol) in human immunodeficiency virus type 1 (HIV-1) display a dominant effect on replicative fitness and drug response. Virology. 2008; 378:272–281. [PubMed: 18599104]
13. Ho SK, Perez EE, Rose SL, Coman RM, Lowe AC, Hou W, Ma C, Lawrence RM, Dunn BM, Sleasman JW, Goodenow MM. Genetic determinants in HIV-1 Gag and Env V3 are related to viral response to combination antiretroviral therapy with a protease inhibitor. AIDS. 2009; 23:1631–1640. [PubMed: 19625947]
14. Lambert-Niclot S, Flandre P, Malet I, Canestri A, Soulie C, Tubiana R, Brunet C, Wirden M, Katlama C, Calvez V, Marcelin AG. Impact of gag mutations on selection of darunavir resistance mutations in HIV-1 protease. J Antimicrob Chemother. 2008; 62:905–908. [PubMed: 18765410]
15. Dam E, Quercia R, Glass B, Descamps D, Launay O, Duval X, Krausslich HG, Hance AJ, Clavel F. Gag mutations strongly contribute to HIV-1 resistance to protease inhibitors in highly drug-experienced patients besides compensating for fitness loss. PLoS Pathog. 2009; 5:e1000345. [PubMed: 19300491]
16. Klabe RM, Bacheler LT, Ala PJ, Erickson-Viitanen S, Meek JL. Resistance to HIV protease inhibitors: a comparison of enzyme inhibition and antiviral potency. Biochemistry. 1998; 37:8735–8742. [PubMed: 9628735]
17. Prabu-Jeyabalan M, Nalivaika E, Schiffer CA. How does a symmetric dimer recognize an asymmetric substrate? A substrate complex of HIV-1 protease. J Mol Biol. 2000; 301:1207–1220. [PubMed: 10966816]
18. Pettit SC, Henderson GJ, Schiffer CA, Swanstrom R. Replacement of the P1 amino acid of human immunodeficiency virus type 1 Gag processing sites can inhibit or enhance the rate of cleavage by the viral protease. J Virol. 2002; 76:10226–10233. [PubMed: 12239298]
19. Doyon L, Croteau G, Thibeault D, Poulin F, Pilote L, Lamarre D. Second locus involved in human immunodeficiency virus type 1 resistance to protease inhibitors. J Virol. 1996; 70:3763–3769. [PubMed: 8648711]
20. Dunn BM, Gustchina A, Wlodawer A, Kay J. Subsite preferences of retroviral proteinases. Methods Enzymol. 1994; 241:254–278. [PubMed: 7854181]
21. Bally F, Martinez R, Peters S, Sudre P, Telenti A. Polymorphism of HIV type 1 gag p7/p1 and p1/p6 cleavage sites: clinical significance and implications for resistance to protease inhibitors. AIDS Res Hum Retroviruses. 2000; 16:1209–1213. [PubMed: 10957718]
22. Saunders MJ, Kim H, Woods TA, Nolan JP, Sklar LA, Edwards BS, Graves SW. Microsphere-based protease assays and screening application for lethal factor and factor Xa. Cytometry A. 2006; 69:342–352. [PubMed: 16604538]
23. Morrison JF. Kinetics of the reversible inhibition of enzyme-catalysed reactions by tight-binding inhibitors. Biochim Biophys Acta. 1969; 185:269–286. [PubMed: 4980133]
24. Giffin MJ, Heaslet H, Brik A, Lin YC, Cauvi G, Wong CH, McRee DE, Elder JH, Stout CD, Torbett BE. A copper(I)-catalyzed 1,2,3-triazole azide-alkyne click compound is a potent inhibitor of a multidrug-resistant HIV-1 protease variant. J Med Chem. 2008; 51:6263–6270. [PubMed: 18823110]
25. Kuckuck FW, Edwards BS, Sklar LA. High Throughput Flow Cytometry. Interface. 2001; 90:83–90.
26. Surawski PP, Battersby BJ, Lawrie GA, Ford K, Ruhmann A, Marcon L, Kozak D, Trau M. Flow cytometric detection of proteolysis in peptide libraries synthesised on optically encoded supports. Mol Biosyst. 2008; 4:774–778. [PubMed: 18563252]
27. Harper S, Speicher DW. Expression and purification of GST fusion proteins. Curr Protoc Protein Sci Chapter 6. 2008; (Unit 6):6.
28. Nagai T, Ibata K, Park ES, Kubota M, Mikoshiba K, Miyawaki A. A variant of yellow fluorescent protein with fast and efficient maturation for cell-biological application. Nature. 2001; 20:1585–1588.

29. Shaner NC, Steinbach PA, Tsien RY. A guide to choosing fluorescent proteins. Nat Methods. 2005; 2:905–909. [PubMed: 16299475]
30. Zacharias DA, Violin JD, Newton AC, Tsien RY. Partitioning of lipid-modified monomeric GFPs into membrane microdomains of live cells. Science. 2002; 296:913–916. [PubMed: 11988576]
31. Pettit SC, Henderson GJ, Schiffer CA, Swanstrom R. Replacement of the P1 amino acid of human immunodeficiency virus type 1 Gag processing sites can inhibit or enhance the rate of cleavage by the viral protease. J Virol. 2002; 76:10226–10233. [PubMed: 12239298]
32. Lee SK, Harris J, Swanstrom R. A strongly transdominant mutation in the human immunodeficiency virus type 1 gag gene defines an Achilles heel in the virus life cycle. J Virol. 2009; 83:8536–8543. [PubMed: 19515760]
33. Nalam MN, Schiffer CA. New approaches to HIV protease inhibitor drug design II: testing the substrate envelope hypothesis to avoid drug resistance and discover robust inhibitors. Curr Opin HIV AIDS. 2008; 3:642–646. [PubMed: 19373036]
34. Buhler B, Lin YC, Morris G, Olson AJ, Wong CH, Richman DD, Elder JH, Torbett BE. Viral evolution in response to the broad-based retroviral protease inhibitor TL-3. J Virol. 2001; 75:9502–9508. [PubMed: 11533212]
35. Markowitz M, Mo H, Kempf DJ, Norbeck DW, Bhat TN, Erickson JW, Ho DD. Selection and analysis of human immunodeficiency virus type 1 variants with increased resistance to ABT-538, a novel protease inhibitor. J Virol. 1995; 69:701–706. [PubMed: 7815532]
36. Muzammil S, Ross P, Freire E. A major role for a set of non-active site mutations in the development of HIV-1 protease drug resistance. Biochemistry. 2003; 42:631–638. [PubMed: 12534275]
37. Myint L, Matsuda M, Matsuda Z, Yokomaku Y, Chiba T, Okano A, Yamada K, Sugiura W. Gag non-cleavage site mutations contribute to full recovery of viral fitness in protease inhibitor-resistant human immunodeficiency virus type 1. Antimicrob Agents Chemother. 2004; 48:444–452. [PubMed: 14742193]
38. Mayr LM, Bojanic D. Novel trends in high-throughput screening. Curr Opin Pharmacol. 2009; 9:580–588. [PubMed: 19775937]
39. Zhang JH, Chung TD, Oldenburg KR. A Simple Statistical Parameter for Use in Evaluation and Validation of High Throughput Screening Assays. J Biomol Screen. 1999; 4:67–73. [PubMed: 10838414]
40. Copeland RA. Mechanistic considerations in high-throughput screening. Anal Biochem. 2003; 320:1–12. [PubMed: 12895464]
41. Shoichet BK. Screening in a spirit haunted world. Drug Discov Today. 2006; 11:607–615. [PubMed: 16793529]

Abbreviations and Textual Footnotes

HAART	highly active anti-retroviral therapy
HIV-1	human immunodeficiency virus 1
CE-CBA	cleavage enzyme - cytometric bead array
FSA	fluorogenic substrate assay
PAGE	polyacrylamide gel electrophoresis
MALDI MS	matrix-assisted laser desorption/ionization mass spectrometry
HTS	high-throughput screening
HPLC	high-pressure liquid chromatography
PR	protease
Gag	group-specific antigen
GST	glutathione S-transferase

mV	mVenus
MA	matrix
CA	capsid
NC	nucleocapsid
Thr	thrombin
CS	cleavage site
NCS	non-cleavage site
PI	protease inhibitor
S	substrate
DDM	n-dodecyl beta-D-maltoside
DMSO	dimethyl sulfoxide
SDS	sodium dodecyl sulfate
DTT	dithiothreitol
IPTG	isopropyl-beta-D-thiogalactospyranoside
GSH	glutathione
APV	amprenavir
MCS	multiple cloning site
s.e.m	standard error of mean
s.d	standard deviation
rFU	relative fluorescence units
k_{cat}/K_M	catalytic efficiency

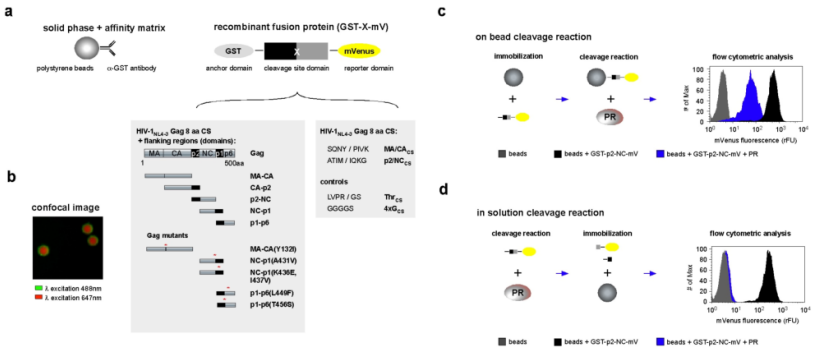

FIGURE 1.

Overview of Cleavage Enzyme – Cytometric Bead Array. (a) Schematic description of the Cleavage Enzyme – Cytometric Bead Array (CE-CBA) platform containing the bead-based anti-GST antibody affinity matrix to which the recombinant fusion protein, GST-X-mV, is coupled. X refers to Gag substrate domains, with endogenous cleavage sites, or Gag cleavage site peptides all encoded from the appropriate HIV-1_{NL4-3} sequence. The two shaded boxes below the GST-X-mV depict Gag domains (left) or the cleavage site for various Gag domains (right) that have been inserted at the site X in GST-X-mV. Gag cleavage site peptides are referred to by the name of the Gag domain followed by a subscript CS, for the cleavage site. (b) Confocal fluorescence image of fluorescent beads (red) coupled to the GST-p2/NC_{CS}-mVs (green). Note the homogeneous distribution of GST-p2/NC_{CS}-mVs and the absence of discrete spots, which would be an indication of protein aggregation or clumping. (c) On bead CE-CBA of GST-p2-NC-mV by HIV-1 PR. The protease recognizes and cleaves the GST-p2-NC-mV at the specific cleavage site liberating the -NC-mV remnant containing mVenus from the bead. Loss of mVenus decreases the fluorescence signal on the bead, which can be quantified utilizing flow cytometry (histogram: right panel). (d) In solution CE-CBA of GST-p2-NC-mV by HIV-1 PR. In this assay GST-p2-NC-mV processing by protease occurs in solution and cleavage products and remaining uncleaved GST-p2-NC-mV is bound to the beads after the enzymatic reaction. Beads with a protease processed GST-p2-NC-mV protease shows the intrinsic fluorescence of the beads only after cleavage and liberation of mVenus (histogram: right panel). All experimental conditions for on-bead and in solution cleavage are fully discussed in Materials and Methods.

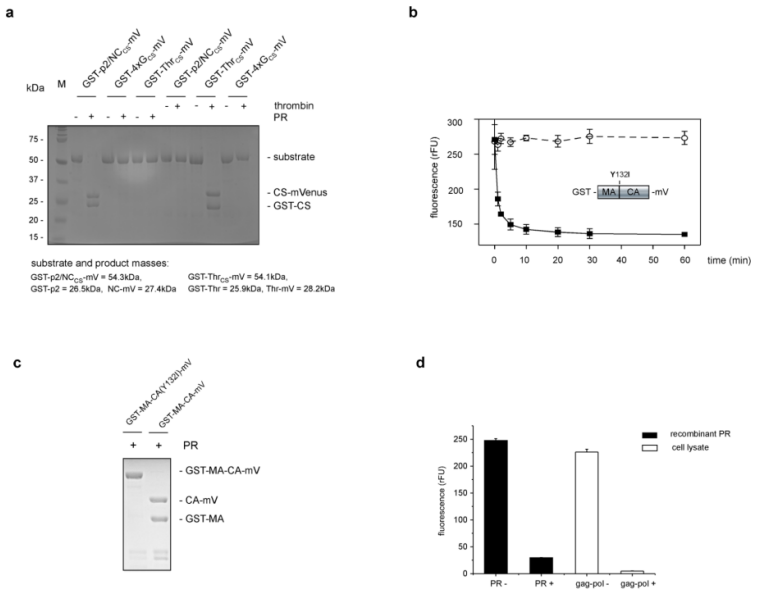

FIGURE 2.

Validation of the fusion protein GST-X-mV. (a) SDS PAGE analysis of the cleavage products of different GST-X-mV fusion proteins after incubation with the protease thrombin or HIV-1 PR. For these studies the X insert was: p2/NC_{CS}, $4xG_{CS}$, or a thrombin cleavage site (Thr). 5 μg of GST-X-mV was incubated with 0.1 μM HIV-1 PR or thrombin for 2 hrs at 37 °C and analyzed by SDS PAGE and coomassie staining. (b) In solution CE-CBA cleavage analysis of Y132I MA-CA mutant. Shown is the time-resolved cleavage analysis of the Y132I MA-CA mutant and wild type MA-CA. GST-X-mV containing the MA-CA protein either with the Y132I MA-CA mutant (○) = GST-MA-CA(Y132I)-mV) or wild type MA-CA (■) = GST-MA-CA(wt)-mV) cleavage site were incubated with HIV-1 PR, samples were removed at the appropriate time, incubated with beads, and then analyzed by flow cytometry. Experimental conditions: sampling over the time; t = 60 min; [S: GST-MA-CA(Y132I)-mV or GST-MA-CA(wt)-mV] = 5 μM; [PR] = 25 nM, T = 37 °C. Values are shown as mean ± s.d. (c) SDS PAGE analysis of the protease-mediated processing of GST-MA-CA-mV and the mutant GST-MA-CA(Y132I)-mV. 5 μg fusion protein (GST-MA-CA-mV or GST-MA-CA(Y132I)-mV was incubated for 3 hrs with 50 μM protease at 37 °C and analyzed by SDS PAGE and coomassie staining. (d) CE-CBA analysis of HIV-1 protease in eukaryotic cell lysates. Plotted values of the fluorescence intensity remaining of the GST-MA/CA_{CS}-mV fusion protein present on the beads (mean ± s.d.). HIV-1 PR was produced in a mammalian cell culture by transfection of HEK 293T cells with pcDNA 3.1 expressing *gag-pol*. GST-MA/CA_{CS}-mV labeled beads were incubated with the cell lysate of the HEK 293T cells or with 300 nM recombinant HIV-1 PR at 37 °C for 1 hr, then analyzed by flow cytometry.

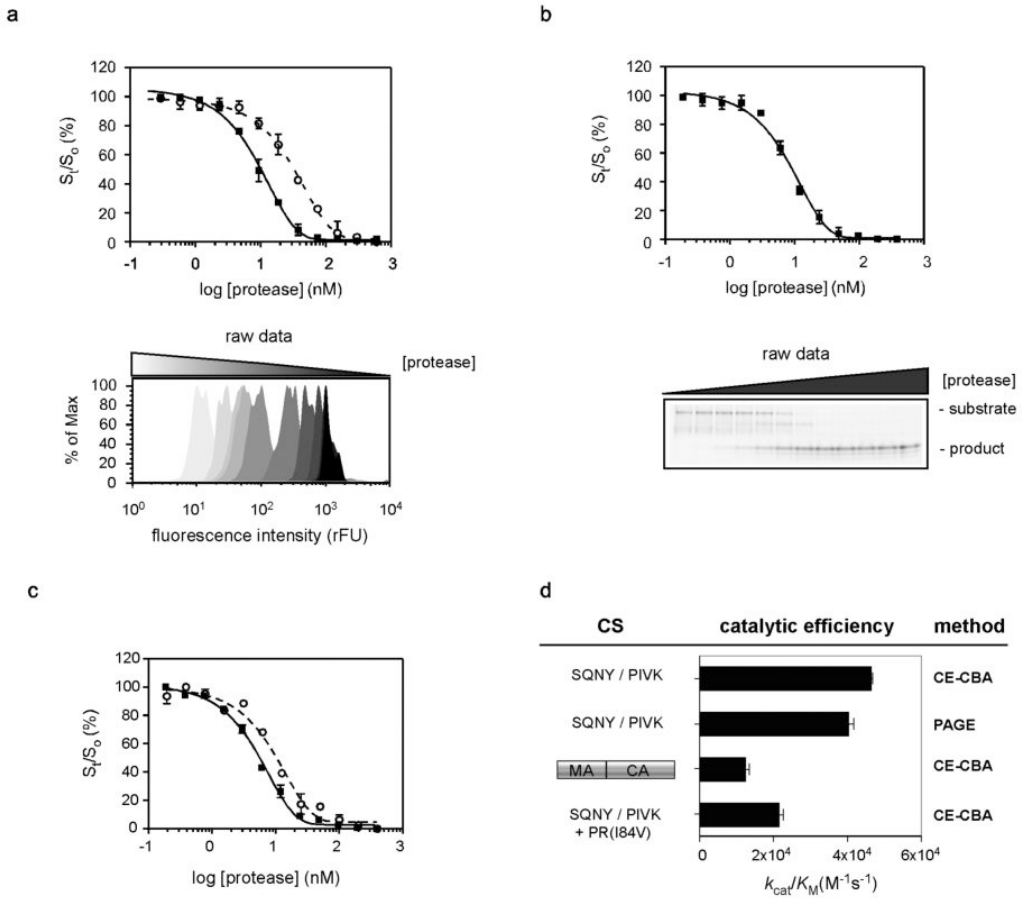

FIGURE 3.

CE-CBA analyses of protease processing of full-length Gag substrates and small peptide cleavage sites. (a) Comparison of catalytic efficiencies obtained from protease processing of Gag MA/CA 8 amino acid cleavage site and Gag MA-CA domains containing the normally embedded cleavage site. Shown are the (S_t/S_o) vs. the log[protease] plotted values (mean ± s.d.) of the in solution CE-CBA cleavage analysis of (■) = GST-MA/CA_{CS}-mV (k_{cat}/K_M= 40.5 ± 1.4 $mM^{-1}s^{-1}$) and (○) = GST-MA-CA-mV (k_{cat}/K_M= 12.4 ± 1.1 $mM^{-1}s^{-1}$) and an example of the data obtained from flow cytometry of cleaved and uncleaved GST-MA-CA-mV resulting from incubation with varying amounts of protease (histogram: lower panel). S_t refers to relative fluorescence intensity of sample after protease addition and S_o = relative fluorescence intensity of sample before protease addition. The curve corresponds to the fit of equation as discussed in Methods and allows calculation of the catalytic efficiency, k_{cat}/K_M. Experimental conditions: t = 30 min; [S: GST-MA/CA_{CS}-mV or GST-MA-CA-mV] = 10 nM; [PR] = 0.3 - 600 nM, T = 37 °C. The raw data presented represents an overlay of the single flow cytometric measurements, where the decreasing fluorescence signal is the result of more cleavage resulting from increased protease concentration. (b) Shown is the protease-mediated GST-MA/CA_{CS}-mV (k_{cat}/K_M= 46.6 ± 0.5 $mM^{-1}s^{-1}$) cleavage analysis by native PAGE. Lower panel is a digital image of the PAGE gel showing cleaved and uncleaved GST-MA/CA-mV resulting from incubation with increasing amounts of protease. Experimental conditions: t = 30 min; [S: GST-MA/CA_{CS}-mV] = 10 nM; [PR] = 0.3 - 600 nM, T = 37 °C. (c) Determination of catalytic efficiencies for wild type and I84V PI-resistant proteases. The k_{cat}/K_M values for the wild type (■) (k_{cat}/K_M= 40.5 ± 1.4 $mM^{-1}s^{-1}$) and I84V (○) (k_{cat}/K_M= 22.0 ± 1.1 $mM^{-1}s^{-1}$) PI-resistant proteases were determined as

described in a, through in solution CE-CBA analysis. Experimental conditions: t = 32 min; [S: GST-MA/CA_{CS}-mV] = 10 nM; [PR] = 0.3 - 600 nM, T = 37 °C). (d) Comparison of the catalytic efficiency values of all Gag cleavage and protease combinations shown in Figures a, b, and c. All reactions reported in a, b, and c were undertaken using concentrations of substrates well below K_M, where the appearance of the product is a pseudo first order process. Results are from a series of three independent experiments with k_{cat}/K_M values presented as mean ± s.e.m.

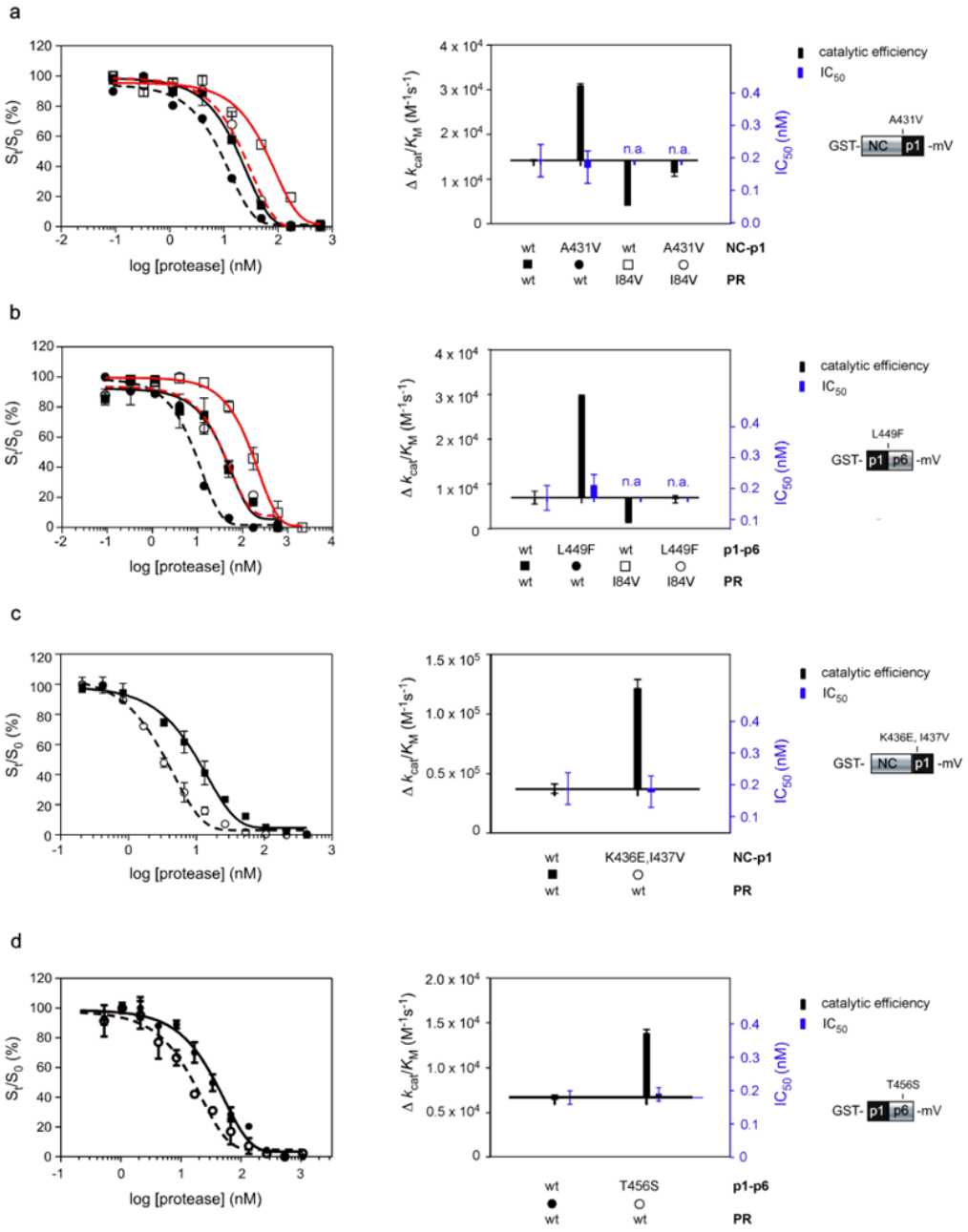

FIGURE 4.

Comparison of the catalytic efficiency of wild type and drug resistant protease and Gag substrate containing cleavage site, distal cleavage site and non-cleavage site mutations. Shown are the (S_t/S_0) vs. the log[protease] plotted values (mean ± s.d.) of the in solution CE-CBA, left panels. The right panel indicates positive and negative changes relative to the wild type protease and Gag and shown are catalytic efficiency and IC_{50} (mean ± s.e.m.) values. (a) Enzymatic analyses of the wt and I84V protease with the *gag* A431V mutant. (■) = GST-NC-p1(wt)-mV + PR(wt), (●) = GST-NC-p1(A431V)-mV + PR(wt), (□) = GST-NC-p1(wt)-mV + PR(I84V), (○) = GST-NC-p1(A431V)-mV + PR(I84V). Experimental conditions: t = 45 min; [S] = 10 nM; [PR] = 0.1 - 600 nM; T = 25 °C. (b) Enzymatic analyses of the wt and I84V protease with the *gag* L449F mutant. (■) = GST-p1-p6(wt)-mV

+ PR(wt), (●) = GST- p1-p6(L449F)-mV + PR(wt), (□) = GST- p1-p6(wt)-mV + PR(I84V), (○) = GST- p1-p6(L449F)-mV + PR(I84V). Experimental conditions: t = 45 min; [S] = 10 nM; [PR] = 0.1 - 2100 nM; T = 25 °C. (c) The distal cleavage site mutations K436E and I437V contribute to increased catalytic efficiency. (■) = GST-NC-p1(wt)-mV, (○) = GST-NC-p1(K436E, I437V)-mV. Experimental conditions: t = 30 min; [S] = 10 nM; [PR] = 0.2 - 425 nM; T = 37 °C. (d) Enzymatic characterization of the non-cleavage site mutation T456S. (●) = GST-p1-p6(wt)-mV, (○) = GST-p1-p6(T456S)-mV. Experimental conditions: t = 50 min; [S] = 10 nM; [PR] = 0.5 - 1100 nM; T = 25 °C.

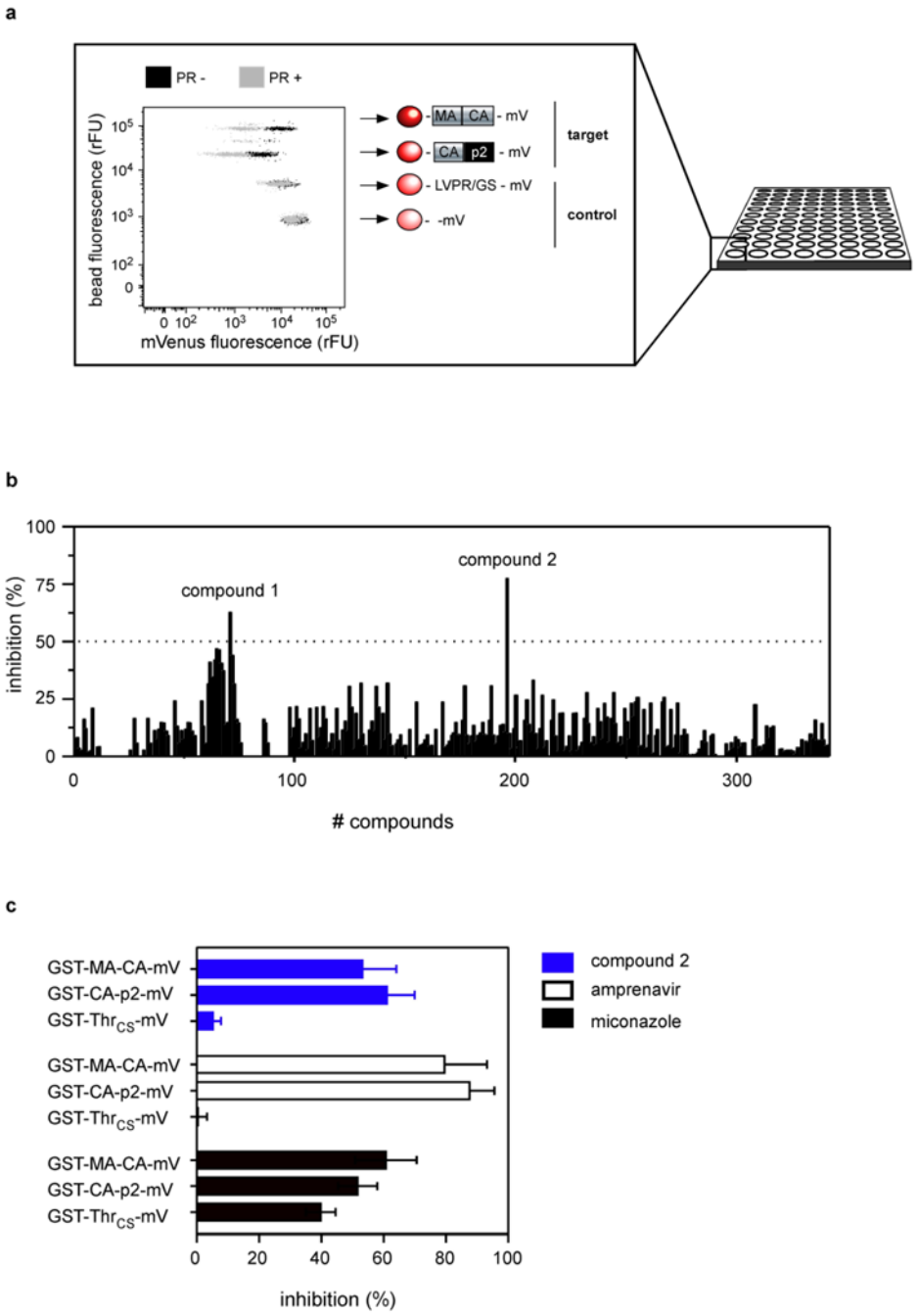

FIGURE 5.

Demonstration of parallel (multiplexed) monitoring and high-throughput screen utilizing CE-CBA. (a) The bivariant dot-plot shows 4 different bead populations in two different states, before and after incubation with HIV-1 PR. The experimental strategy has been established to identify Gag inhibitors, which target specific cleavage site sites or non-cleavage site locations of the Gag substrate. In the example shown in Figure 5, each of the 4 bead populations can be identified by their distinct red fluorescence intensities utilizing flow cytometry. The two upper positions are beads coupled with the Gag substrates GST-MA-CA-mV or GST-CA-p2-mV. The two lower bead populations are controls monitoring off-target activity for inhibitor screening. GST-Thr$_{CS}$-mV (cleavage site: LVPR/GS) serves as a

control for non-specific protease cleavage and the last bead position is a GST-X-mV protein without cleavage site for monitoring fluorescence changes by intrinsic fluorescence of compounds and compound interference with the matrix of the beads. This multiplexed CE-CBA was carried out in 96-well or 384-well plates using an automated HTS robotic platform coupled with a FACSCanto II flow cytometer. (b) Example of a multiplexed CE-CBA HTS using the set up displayed in (a) without the thrombin control and a combinatorial small-compound library containing ~ 340 compounds. Two compounds showed inhibitory activity over 50 %. (c) Example of a inhibitor hit validation using multiplex CE-CBA. Hits from the screen shown in (b) were applied on a CE-CBA analysis using 4 GST-X-mV substrates as shown in (a). In addition a well-known promiscuous inhibitor miconazole and a standard PI, amprenavir, were tested and the inhibition activity displayed (mean ± s.e.m.). Compound 1 did not reproduce inhibition activity (data not shown). The fluorescence of the control containing no cleavage site was not impaired. Only amprenavir and compound 2 showed specific inhibition of the cleavage reaction of both Gag substrates, but not of the thrombin substrate, thereby indicating PI specificity for compound 2.